Monatshefte für Chemie 130, 1319–1331 (1999)

Monatshefte für Chemie
Chemical Monthly
© Springer-Verlag 1999
Printed in Austria

Photophysics and *(E/Z)*-Photoisomerization of 1-(2-Naphthyl)-2-(2-benzothiazolyl)ethenes

Tarek A. Fayed* and **Safaa El-Din H. Etaiw**

Department of Chemistry, Faculty of Science, Tanta University, Tanta, Egypt

Summary. The fluorescence properties and photoisomerization of *trans* isomers of 1-(2-naphthyl)-2-(2-benzothiazolyl)ethene (1,2-*NBE*) and its benzothiazolium cation (1,2-*NBEI*) have been studied in different solvents. The solvent dependence of the absorption and fluorescence maxima, specially in case of 1,2-*NBEI*, reflects an intramolecular charge transfer character in the lowest excited singlet state. Both fluorescence and photoisomerization yields depend on solvent and excitation wavelength. Introduction of a positive charge significantly affects the photophysical and photochemical properties of the investigated compounds. The spectral maxima of 1,2-*NBEI* are largely red shifted, and the fluorescence is strongly quenched compared to 1,2-*NBE*. Also, a reverse thermal isomerization competes with the photochemical reaction. The kinetics of the thermal *cis*→*trans* isomerization have been studied, and its mechanism is discussed. In addition, the fluorescence and photoisomerization quenching by amines and ferrocene has been investigated. The *Stern-Volmer* quenching constants depend on the structure of the fluorophore and the ionization potential of the amine as well as on the solvent polarity. The data show that amines quench the fluorescence more efficiently than the photoisomerization, suggesting a contribution from the excited triplet state to the isomerization reaction.

Keywords. Benzothiazolium; Intramolecular charge transfer; Photoisomerization; Thermal isomerization; Quenching.

Photophysik und (*E*/*Z*)-Photoisomerisierung von 1-(2-Naphthyl)-2-(2-benzothiazolyl)ethenen

Zusammenfassung. Die Fluoreszenzeigenschaften und die Photoisomerisierung der *trans*-Isomeren von 1-(2-Naphthyl)-2-(2-benzothiazoyl)ethen (1,2-*NBE*) und seinem Benzothiazoliumkation (1,2-*NBEI*) wurden in verschiedenen Lösungsmitteln untersucht. Die Lösungsmittelabhängigkeit der Absorption und der Fluoreszenzmaxima, speziell im Fall von 1,2-*NBEI*, zeigt *Charge-transfer*-Charakter des niedrigsten angeregten Singlettzustands. Sowohl Fluoreszenz- als auch Photoisomerisationsausbeute hängen vom Lösungsmittel und von der Anregungswellenlänge ab. Die Einführung einer positiven Ladung beeinflußt die photophysikalischen und photochemischen Eigenschaften der untersuchten Verbindungen maßgeblich. Die spektralen Maxima von 1,2-*NBEI* werden stark ins Rote verschoben, und die Fluoreszenz wird im Vergleich zu 1,2-*NBE* stark gelöscht. Eine entgegengesetzte thermische Isomerisierung konkurriert mit der photophysikalischen Reaktion. Die Kinetik der thermischen *cis-trans*-Isomerisierung wurde untersucht und ihr Mechanismus wird diskutiert. Zusätzlich wurde die Löschung von Fluoreszenz und Photoisomerisierung durch Amine und

---

* Corresponding author

Ferrocen studiert. Die *Stern*-*Volmer*-Löschkonstanten hängen von der Struktur des Fluorophors und dem Ionisierungspotential des Amins sowie von der Polarität des Lösungsmittels ab. Die gewonnenen Daten zeigen, daß Amine die Fluoreszenz effizienter löschen als die Photoisomerisierung: das legt die Beteiligung eines Beitrags des angeregten Triplettzustands an der Isomerisierungsreaktion nahe.

Introduction

The photochemistry of 1,2-diarylethylenes (*Ar*-CH=CH-$\bar{Ar}$, $\bar{Ar}$ = naphthyl) has received much attention [1, 2] because of the two effects exerted by the naphthyl substituent in 2-styrylnaphthalene: (*i*) the lowest excited state of the aromatic moiety noticeably increases the fluorescence quantum yield but decreases the photoisomerization yield at room temperature and (ii) the strong steric interaction between the naphthyl group and the ethylenic hydrogen is important in determining the mixtures of conformers originating from rotation of the naphthyl group about a *quasi*-single bond between the aryl group and the ethylenic carbon atom.

Many aza analogues of *trans*-2-styrylnaphtalene have also been investigated [3–6]. It was found that the n–π^*-states introduced by the nitrogen atom significantly affect the photophysical and photochemical properties of such compounds. However, much less is known about the photochemistry of diarylethylenes bearing heterocyclic rings containing sulfur [7–9]. Thus, the aim of the present study is to report on the photophysical properties as well as the photochemical $E \rightleftharpoons Z$ (*trans*-*cis*) isomerization of 1-(2-naphthyl)-2-(2-benzothiazolyl)ethene (1,2-*NBE*, see Scheme 1). To show the influence of the positive charge on the ground and excited states, the benzothiazolium iodide derivative (1,2-*NBEI*) was also studied. The importance of benzothiazole derivatives is due to their biological activity and their use as pesticides [10], growth regulating substances [11], and intermediates for dyes, plant protectants, and pharmaceuticals [12].

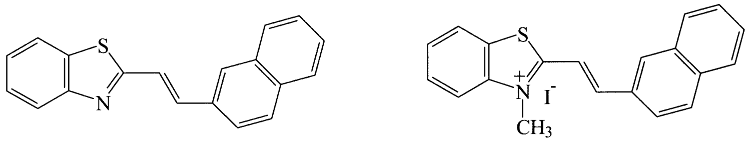

1,2-NBE 1,2-NBEI

Scheme 1

Results and Discussion

Spectral characteristics

Figure 1 shows the absorption, fluorescence, and excitation spectra of 1,2-*NBE* and 1,2-*NBEI* in ethanol as an example; the corresponding spectral data are summarized in Table 1. The absorption spectra of 1,2-*NBE* exhibit vibrational structure, specially in nonpolar solvents such as cyclohexane, but those of 1,2-*NBEI* are characterized by a broad structureless long-wavelength band in the visible region. The fluorescence excitation spectra of 1,2-*NBE* coincide with the absorption spectra,

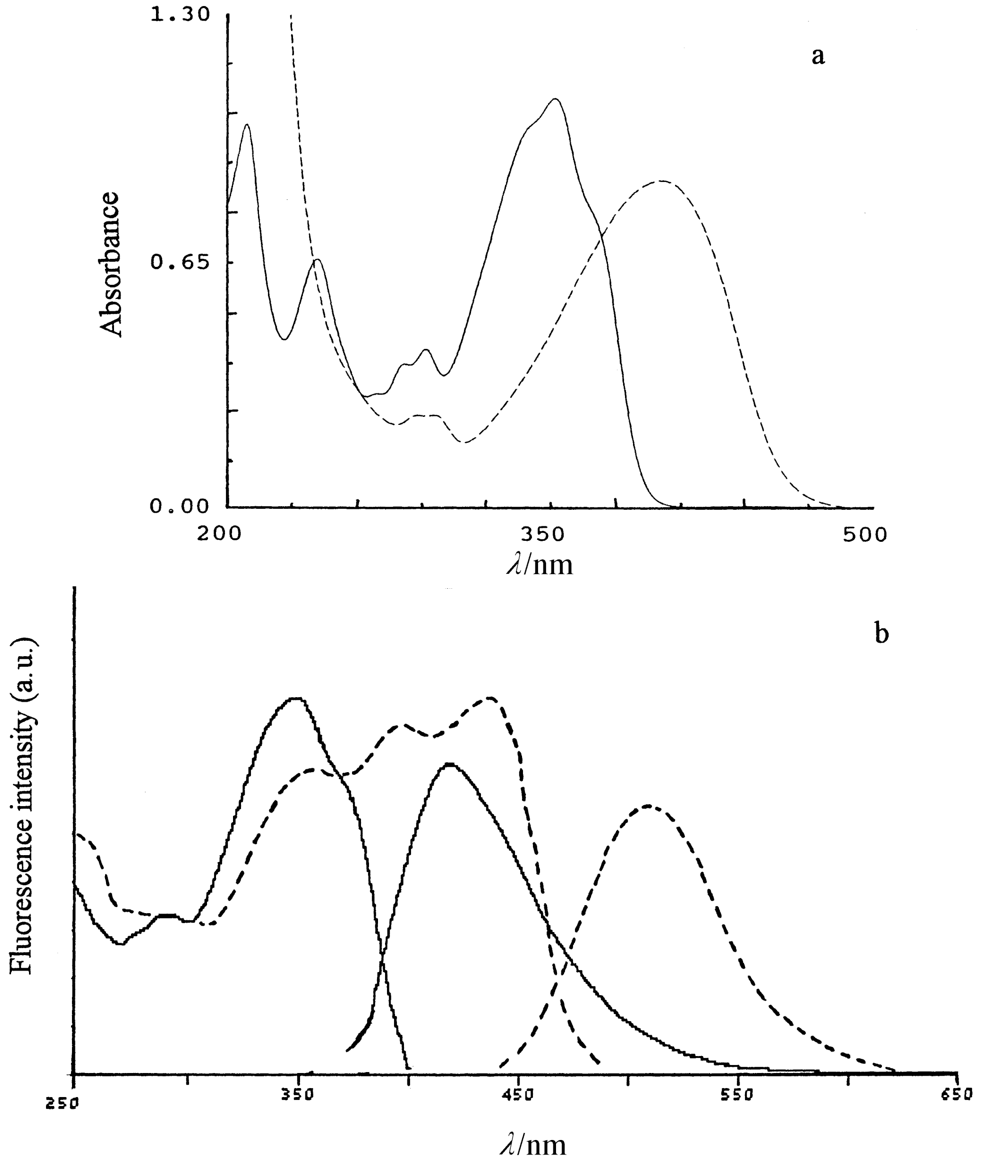

Fig. 1. (a) Absorption spectra of 1,2-*NBE*(—) and 1,2-*NBEI* (- - -) in ethanol; (b) corresponding fluorescence (λ_{ex}: absorption maximum) and fluorescence excitation spectra

but those of 1,2-*NBEI* do not. The long wavelength absorption bands are probably due to π–π^* transitions as indicated by the larger molar absorption coefficients (ε_{max} in the range of $1.8–3.9 \times 10^4 M^{-1} \cdot cm^{-1}$). Table 1 shows that the introduction of a positive charge on the nitrogen atom of 1,2-*NBE* leads to a large red shift of both the absorption and emission maxima (*ca.* 50 and 100 nm, respectively). Whereas the absorption maximum of 1,2-*NBE* is insensitive to solvent polarity, that of the emission suffers a red shift as the solvent polarity is increased, thus indicating an increase in the dipole moment upon excitation. However, for 1,2-*NBEI* in protic solvents an increase of the solvent polarity results in a hypsochromic shift in the

Table 1. Spectral characteristics of 1,2-NBE and 1,2-*NBEI* in different solvents at 25°C

Solvent	1,2-*NBE*			1,2-*NBEI*			
	λ_a (nm)	$\varepsilon_{max}\times10^{-4}$ ($M^{-1}\cdot cm^{-1}$)	$\lambda_f(\lambda_{ex}=350)$ (nm)	λ_a (nm)	$\varepsilon_{max}\times10^{-4}$ ($M^{-1}\cdot cm^{-1}$)	λ_f ($\lambda_{ex}=405$) (nm)	$\Delta\bar{\nu}$ (cm^{-1})
H_2O	–	–	–	395	2.5	516	5936
Methanol	352	3.8	417	400	2.8	511	5431
Ethanol	351	3.7	416	405	1.8	509	5045
n-Butanol	–	–	–	410	1.9	503	4510
CH_3CN	349	3.9	412	399	3.0	515	5646
CH_2Cl_2	352	3.8	414	422	2.8	514	4242
Cyclohexane	350, 361	3.9	403	–	–	–	–

absorption spectra, but a bathochromic shift in the fluorescence spectra. To discuss such solvent effects, the dipole moment changes in the ground and excited states must be taken into consideration. In case of charged donor-acceptor chromophores, here the benzothiazolium cation, the dipole moment changes are due to an intramolecular charge transfer. In the ground state the positive charge is essentially localized on the benzothiazolium moiety, whereas upon excitation the positive charge is more or less shifted to the naphthyl part. The intramolecular charge transfer and the consequent solvent relaxation processes in both the excited and ground states are confirmed by the large *Stokes* shift ($\Delta\bar{\nu}$ ranges from 4242 to $5936\,cm^{-1}$).

The fluorescence quantum yield of 1,2-*NBE* is much higher and more sensitive to the medium in comparison with 1,2-*NBEI* (Table 2). In case of 1,2-*NBE*, the fluorescence yield decreases with increasing solvent polarity. This is probably due to vibronic coupling between the close lying n–π^* and π–π^* states which increases the possibility of nonradiative transitions to deactivate the excited states. However, in polar protic solvents such as alcohols, ϕ_f is lower compared to that in non-

Table 2. Effect of excitation wavelength on the fluorescence characteristics of 1,2-*NBE* and 1,2-*NBEI*

Solvent	1,2-*NBE*					1,2-*NBEI*			
	$\lambda_{ex}=344$ nm		365 nm	382 nm		365 nm		405 nm	
	ϕ_f	λ_f (nm)	ϕ_f	ϕ_f	λ_f (nm)	ϕ_f	λ_f (nm)	ϕ_f	λ_f (nm)
H_2O	–	–	–	–	–	0.0024	–	0.0015	–
Methanol	0.013	417	0.022	0.027	425	0.0026	–	0.0016	–
Ethanol	0.021	416	0.03	0.039	429	0.032	509	0.014	517*
CH_3CN	0.022	412	0.039	0.043	419	0.0033	–	0.0017	–
CH_2Cl_2	0.046	414	0.068	0.091	431	0.0015	514	0.0013	518*
Cyclohexane	0.104	403	0.179	0.189	413	–	–	–	–

* $\lambda_{ex}=465$ nm

hydrogen bonding solvents of similar or even higher polarity such as CH_3CN. This behaviour can be attributed to solute-solvent hydrogen bonding interactions which enhance the nonradiative internal conversion. The fluorescence quantum yield of 1,2-*NBEI* shows a somewhat different dependence, tending to increase with increasing solvent polarity from CH_2Cl_2 to CH_3CN or alcohols. This behaviour can be interpreted on the basis of the fact that in strongly polar solvents the salt exists mostly in a dissociated form; in less polar solvents, it forms ion-pairs. Thus, the interaction of the iodide anion with the *trans* isomer of the cation is different in both cases. The ion-pair nature of 1,2-*NBEI* in CH_2Cl_2 may explains the large red shift in the absorption maximum compared to CH_3CN. The fluorescence quenching of 1,2-*NBEI* may be due to several factors such as *trans/cis* photoisomerization, intramolecular charge transfer from the naphthyl part to the benzothiazolium moiety, induced heavy atom intersystem crossing, and anion fluorophore charge transfer process [17]. In fact, the radiationless *trans-cis* photoisomerization is not the main factor causing fluorescence quenching of 1,2-*NBEI* as can be seen from the fact that the photoisomerization quantum yields of both 1,2-*NBE* and its cation in methanol are comparable (Table 3). The intramolecular charge transfer (ICT) induces more efficient radiationless deactivations; therefore, it seems to play a major role in decreasing the fluorescence yield of 1,2-*NBEI*. To give an evidence for the role of the ICT, the iodide counter ion was replaced by the weak electron donor ClO_4^- anion which also has no heavy atom effect. In fact, such a replacement leads to a little enhancement of the fluorescence yield (in methanol, $\phi_f = 0.0026$ and 0.0034 for the I^- and ClO_4^- derivatives, respectively). This experimental result suggests that the induced heavy atom intersystem crossing and the photoinduced electron transfer from the iodide counter ion to the fluorescent cation contribute to a smaller extent to the fluorescence quenching.

Table 3. Solvent and excitation wavelength dependence of the *trans-cis* photoisomerization of 1,2-*NBE* and 1,2-*NBEI* at 25°C

Solvent	1,2-*NBE*								
	$\lambda_{ex} = 334$ (nm)			$\lambda_{ex} = 365$ (nm)			$\lambda_{ex} = 382$ (nm)		
	ϕ_t	ϕ_c	%*cis*	ϕ_t	ϕ_c	%*cis*	ϕ_t	ϕ_c	%*cis*
Methanol	0.15	0.18	78	0.16	0.16	89	0.20	0.18	94
Ethanol	0.15	0.16	76	0.17	0.16	89	0.24	0.13	92
CH_3CN	0.14	0.16	77	0.16	0.17	86	0.25	0.26	85
CH_2Cl_2	0.13	0.13	77	0.19	0.14	88	0.20	0.17	90
Cyclohexane	0.13	0.12	78	0.14	0.13	88	0.26	0.24	85
	1,2-NBEI								
	$\lambda_{ex} = 365$ (nm)			$\lambda_{ex} = 405$ (nm)			$\lambda_{ex} = 436$ (nm)		
	ϕ_t	ϕ_c	%*cis*	ϕ_t	ϕ_c	%*cis*	ϕ_t	ϕ_c	%*cis*
H_2O	0.08	0.18	61	0.13	0.24	74	0.19	0.31	85
Methanol	0.14	0.22	69	0.15	0.30	80	0.20	0.53	85

As can be seen from Table 2, the emission maxima and quantum yields of both 1,2-*NBE* and 1,2-*NBEI* in various solvents at room temperature change with changing excitation wavelength. For example, the fluorescence yield of 1,2-*NBE* in cyclohexane (which gives higher ϕ_f-values) increases from 0.104 at $\lambda_{ex} = 334$ nm to 0.189 at $\lambda_{ex} = 382$ nm, whereas the emission maximum is red-shifted from 403 to 413 nm, respectively. Contrary, the fluorescence yield of 1,2-*NBEI* decreases upon excitation at larger wavelengths. Such a behaviour can be attributed to the existence of different *quasi*-planar conformers for both compounds due to rotation of the naphthyl and/or benzothiazolyl group around the *quasi*-single bond between the aromatic group and the ethylenic carbon atom [18].

Direct $E \rightleftharpoons Z$ (trans/cis) photoisomerization

Figure 2 illustrates the effect of photoirradiation at 365 nm on 1,2-*NBE* in cyclohexane at 25°C. The decrease in the absorbance of the long-wavelength band (at 350 nm) is accompanied by an increase in the absorbance around 220 nm with appearance of isosbestic points at 305, 265, and 243 nm. These changes are ascribed to the photochemical $E \rightleftharpoons Z$ isomerization and the establishment of a photostationary state (PSS). The appearance of well defined isosbestic points indicates that the *trans*-*cis* isomerization process proceeds without side reactions. The composition of the photostationary state (*%cis*) varies with the excitation wavelength in accordance with the relative absorbance of the two isomers (Table 3). With respect to 1,2-*NBEI*, the PSS absorption spectra revert completely back into the original spectra at rates depending on solvent and temperature. Therefore, its photoisomerization reaction could be studied only in water and methanol. In ethanol, CH_3CN, and CH_2Cl_2 the

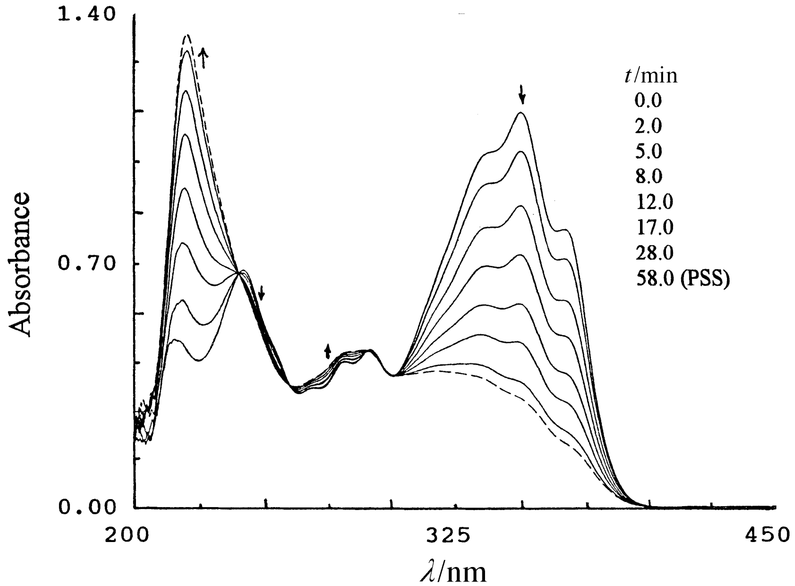

Fig. 2. Effect of photo-irradiation at 365 nm on the absorption spectra of 2.9×10^{-5} *M* 1,2-*NBE* in cyclohexane; the irradiation times at decreasing the absorbance around 350 nm are indicated in the figure

thermal backward $Z \rightarrow E$ reaction is superimposed on the photoisomerization process. The photochemical quantum yields of $E \rightarrow Z$ (ϕ_t) and $Z \rightarrow E$ (ϕ_c) isomerization (Table 3) depend on the irradiation wavelength as well as on the nature of solvent. The shorter the irradiation wavelength, the smaller the quantum yield. This can be explained on the basis of a ground state conformational equilibrium of both compounds as discussed previously. Similar to the fluorescence yield, ϕ_t increases on going from polar protic to polar aprotic solvents. In the case of 1,2-*NBEI* the ϕ_c-values are higher than the corresponding ϕ_t-values due to the additive effect of the thermal back reaction.

Thermal $Z \rightarrow E$ isomerization

Whereas the spectra of the PSS solutions of 1,2-*NBE* are stable at room temperature for more than one week, those of 1,2-*NBEL* revert completely to the spectra of the pure *trans* isomer on standing in the dark at room temperature. The kinetics of the $Z \rightarrow E$ thermal isomerization of 1,2-*NBEI* were measured in different solvents over a suitable temperature range. The lifetime of the *cis* isomer ranges from hours to minutes.

The spectral variations as a result of heating up a PSS methanolic solution of 1,2-*NBEI* as well as the first-order plots of the thermal reaction in ethanol are depicted in Fig. 3. The activation parameters were calculated from the temperature variation of the rate constant ($k_{Z \rightarrow E}$, Table 4). The rate constant at 25°C and the activation parameters depend strongly on the nature of the solvent. The energy of activation (ΔE_a) increases with decreasing $k_{Z \rightarrow E}$ upon changing the solvent from CH_3CN to methanol which indicates an enthalpy controlled reaction. Fig. 4 shows the isokinetic relationship (plot of $\Delta H^{\#}$ *vs.* $\Delta S^{\#}$) for the thermal isomerization of 1,2-*NBEI* in different solvents. The isokinetic temperature (temperature at which each reaction has the same values of rate constant) was calculated from the slope of the correlation as 165°C. the applicability of such a relation indicates that the thermal isomerization follows the same mechanism in various solvents [19]. Furthermore, the observed solvent effects on $k_{Z \rightarrow E}$ suggest that the thermal isomerization of 1,2-*NBEI* proceeds *via* a rotation process around the ethylenic bond, similar to that reported from azobenzenes [20]. It is worthwhile to note that the ICT interaction enhances the single bond character of the central ethylenic bridge which facilitates the rotation process and, therefore, the *cis* to *trans* thermal reaction. Scheme 2 illustrates the rotational mechanism of the thermal isomerization of 1,2-*NBEI*.

Fluorescence and photoisomerization quenching

To gain information about the mechanism of the *trans-cis* photoisomerization, the fluorescence and photoisomerization quenching of both compounds was studied in CH_3CN and cyclohexane using *TEA* and *DABCO* as quenchers. Neither the absorption nor the fluorescence spectra change with increasing amine concentration, indicating the absence of ground or excited state complex formation. Table 5 presents the *Stern-Volmer* quenching constants (K_{SV}) of fluorescence quenching, whereas Fig. 5 shows the corresponding plots. A comparison of the quenching

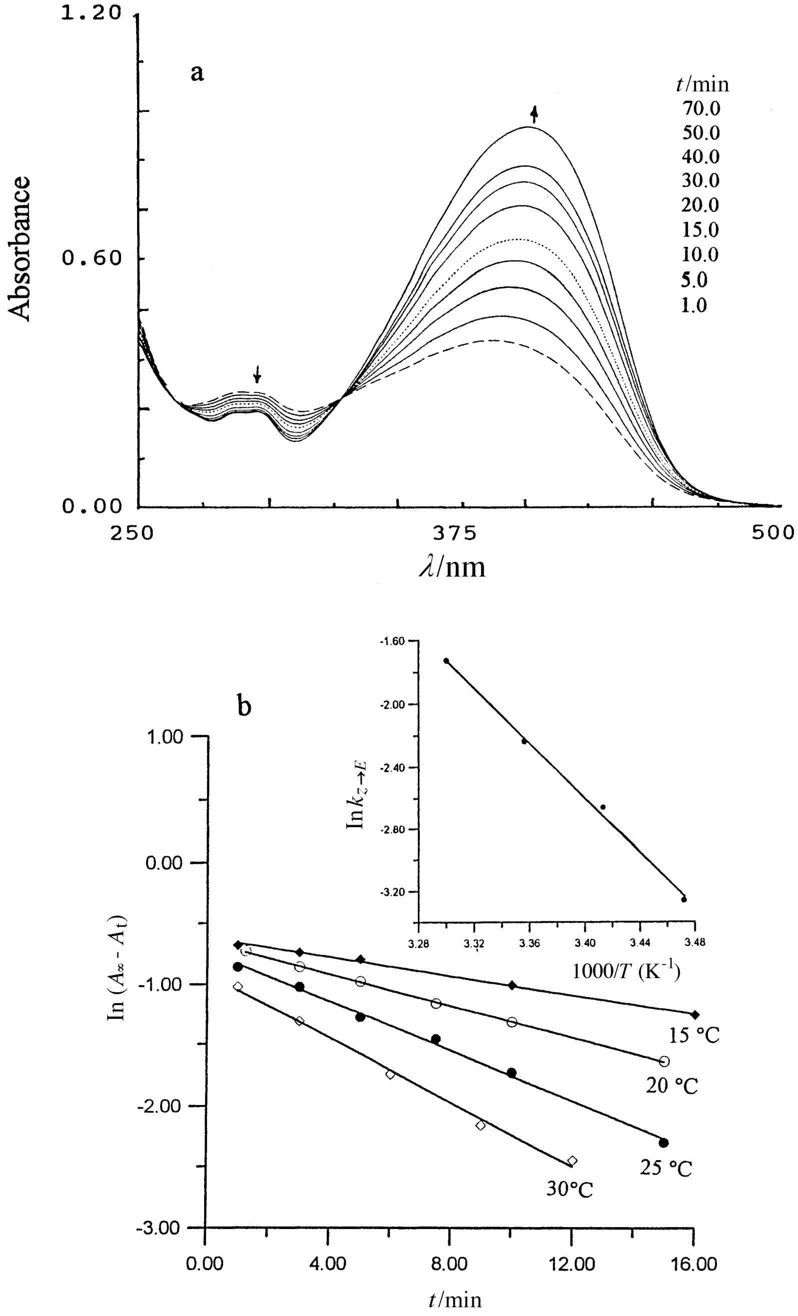

Fig. 3. (a) Change in the absorption spectra of a photostationary state methanolic solution of 1,2–*NBEI* upon heating at 40°C; the heating times are indicated; (b) first-order plots for the thermal *cis*→*trans* isomerization of 1,2-*NBEI* in ethanol; inset: *Arrhenius* plot

constants shows that K_{SV} increases with decreasing ionization potential of the amine quencher or upon introduction of a positive charge on 1,2-*NBE*. Although the half-wave reduction potentials of 1,2-*NBE* and its cation have not been measured, it is likely that the reduction potential of 1,2-*NBEI* is lower than that of the neutral

Table 4. Rate constant ($k_{Z\rightarrow E}$) of the thermal isomerization of 1,2-*NBEI* (at 25°C) and activation parameters as well as the frequency factor in different solvents

Solvent	$k_{Z\rightarrow E}$ (min^{-1})	$t_{1/2}$ (min)	ΔE_a (kJ/mol)	$\Delta H^{\#}$ (kJ/mol)	$\Delta G^{\#}$ (kJ/mol)	$\Delta S^{\#}$ (J/mol · K)	$A\times10^{-12}$ (s^{-1})
Methanol	0.0065	106.0	83.60	81.80	85.5	−20.0	2.98
Ethanol	0.107	6.5	71.04	68.60	78.4	−40.0	0.31
CH_3CN	0.248	3.0	52.39	49.98	75.7	−90.0	0.003

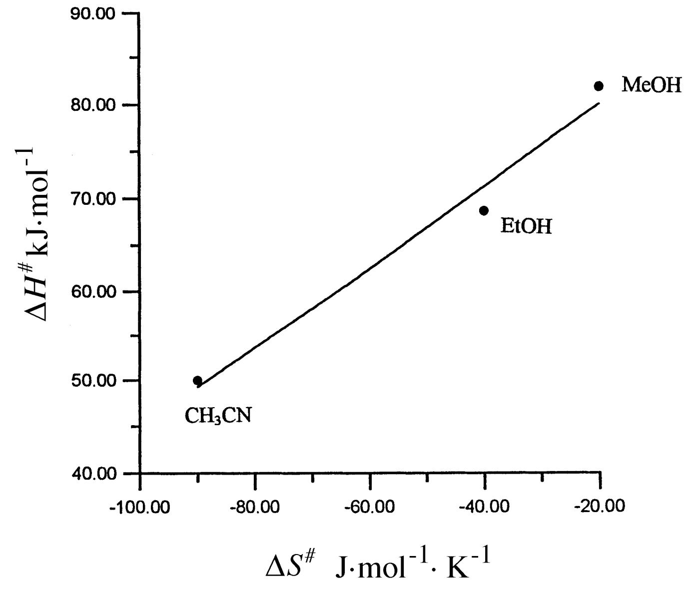

Fig. 4. Iso-kinetic relationship for the thermal isomerization of 1,2-*NBEI*

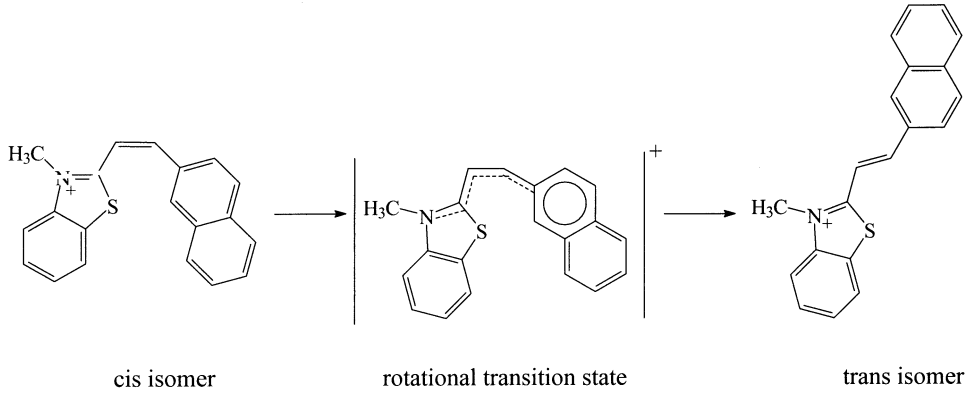

Scheme 2

Table 5. Quenching constants (K_{SV}) of the fluorescence quenching of 1,2-*NBE* and 1,2-*NBEI* by amines

Compound	Solvent	Quencher	K_{SV} (M^{-1})
1,2-*NBE*	Cyclohexane	*DABCO*	7.9
		TEA	3.2
	CH_3CN	*DABCO*	5.3
		TEA	2.4
1,2-*NBEI*	CH_3CN	*DABCO*	13.8
		TEA	7.7

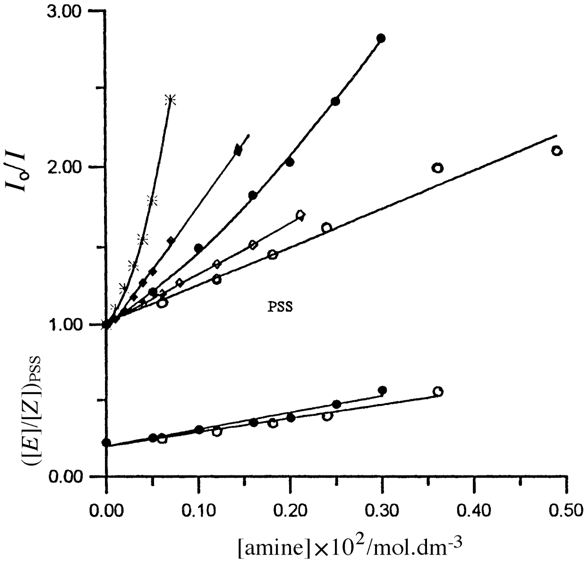

Fig. 5. *Stern-Volmer* plots for the fluorescence and photoisomerization quenching of 1,2-*NBE* by *DABCO* (◆) and *TEA* (●) in cyclohexane and in CH_3CN (open symbols) as well as that of 1,2-*NBEI* by *DABCO* (∗) in CH_3CN

1,2-*NBE*. This behaviour may reflect the electron transfer nature of the fluorescence quenching. Figure 5 also shows the strong influence of solvents on the quenching process. In non-polar cyclohexane, the quenching constant is higher than that in CH_3CN.

Taking the values of $([E]/[Z])_{PSS}$ as a measure of the *trans-cis* geometrical interconversion in the presence of quenchers, it can be observed that amines quench the fluorescence of 1,2-*NBE* efficiently than the photoisomerization reaction (Fig. 5). This is consistent with the contribution of the excited triplet state to the photoisomerization process [4, 6]. To get more information, the effect of ferrocene on the fluorescence and the composition of the photostationary state is studied in ethanol. Unfortunately, the strong overlap between the absorption

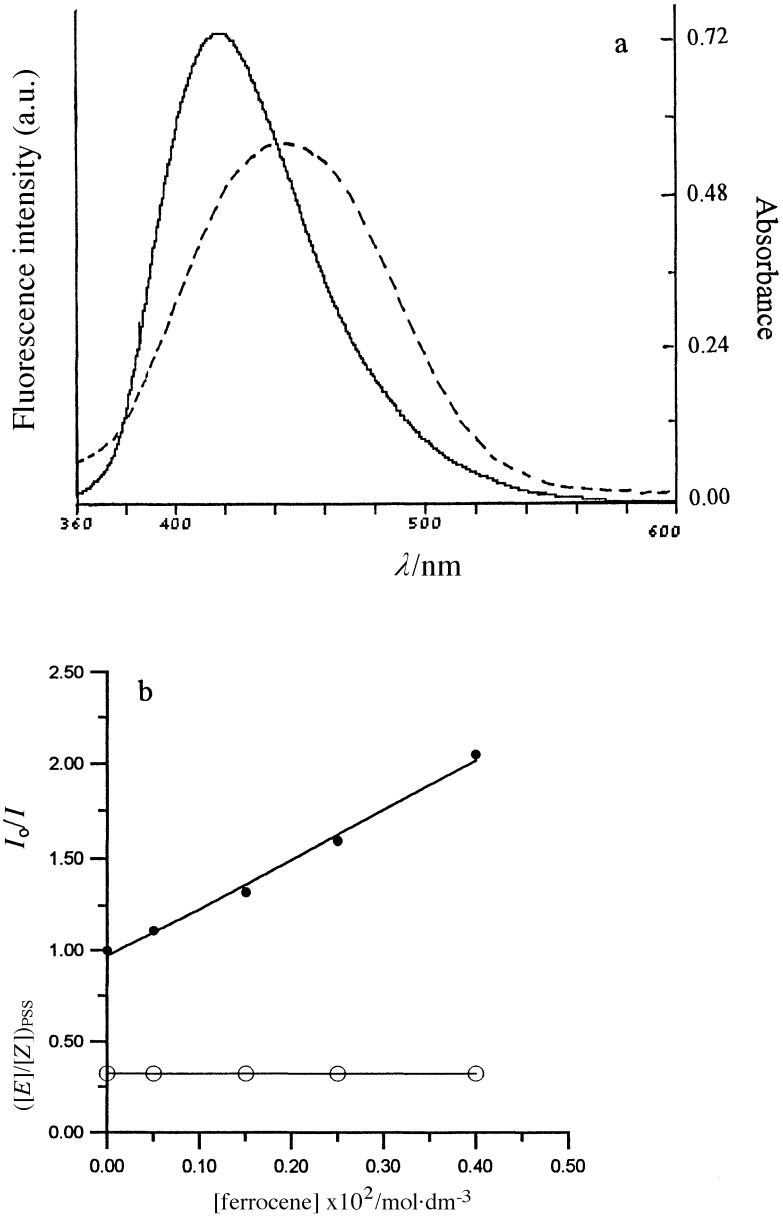

Fig. 6. (a) Overlap between the absorption spectrum of ferrocene (—) and the emission spectrum of 1,2-*NBE* (- - -) in ethanol; (b) *SV*-plots for fluorescence (●) and photoisomerization (○) quenching of 1,2-*NBE* by ferrocence in ethanol

spectrum of ferrocene and the emission spectrum of 1,2-*NBE* (Fig. 6) leads to an efficient radiationless energy transfer interaction ($K_{SV} = 261\,M^{-1}$). Since the triplet state is populated *via* the excited singlet state, increasing the ferrocene concentration has almost no effect on the composition of the photostationary state. However, the contribution of the triplet state to the photoisomerization process can be supported by similarities in the effect of solvents on both ϕ_f and ϕ_t.

Experimental

1-(2-Naphthyl)-2-(2-benzothiazolyl)ethene (1,2-*NBE*) was prepared by condensation of 2-methylbenzothiazole with β-naphthaldehyde as reported previously [13] and recrystallized twice from ethanol. The product was characterized by elemental analysis, IR, and UV/Vis spectral measurements. The elemental analysis data for $C_{19}H_{13}NS$ agree with the calculated values. The IR spectrum shows bands at 1608 and $1590\,cm^{-1}$ as well as at $942\,cm^{-1}$ characteristic for the ethylenic C=C and C–H groups. The corresponding benzothiazolium iodide (1,2-*NBEI*) was obtained by heating equimolar quantities of 1,2-*NBE* and methyl iodide in ethanol for 1 h under reflux to yield orange crystals. The elemental analysis data again correspond to the theoretical values. The IR spectrum shows bands at 1626 and $959\,cm^{-1}$ characteristic for the ethylenic double bond and the C–H group of *trans* olefins, respectively. Also, the spectrum reveals vibrational bands at 1217 and $1202\,cm^{-1}$ resulting from the quaternary $C–N^+$ group.

Commercially available 2-methylbenzothiazole (Fluka), β-naphthaldehyde (Aldrich), and methyl iodide (Aldrich) were used without further purification. Triethylamine (*TEA*, Aldrich) was distilled under vacuum, and 1,4-diazabicyclo[2, 2, 2]octane (*DABCO*, Aldrich) was sublimed before use. All solvents were of spectroscopic grade (from Aldrich or Merck) and used as received. Water was doubly distilled.

The absorption spectra were recorded on a Shimadzu 3101 PC scanning spectrophotometer. Emission spectra were measured using a Perkin-Elmer LS 50B luminescence spectrometer. The fluorescence quantum yields (ϕ_f) were determined at room temperature using 9,10-diphenylanthracene ($\phi_f = 0.95$ in ethanol) as a standard [14], taking into account the effect of the refractive index of solvents. The photoisomerization quantum yields as well as the composition of the photostationary states were calculated as discribed previously [15]. The light intensity was determined using ferrioxalate actinometry [16]. To determine the thermal isomerization rate constant, irradiation was performed at a pre-adjusted temperature (within the range of 10–40°C depending on the solvent) in a $3\,cm^3$ quartz cell using 365 nm light. Irradiation was stopped after reaching the photostationary state, and the sample was moved quickly to a temperature-controlled spectrophotometer cell holder. The absorbance changes were followed at the absorption maxima, and the isomerization rate was calculated applying a least-squares fit. The sample concentrations were in the range from 3.0×10^{-5} to $5.0\times10^{-6}\,mol.dm^{-3}$ depending on substance and solvent.

References

[1] Hass E, Fischer G, Fischer E (1973) J Phys Chem **82**: 1638
[2] Bartocci G, Masetti F, Mazzucato U, Spalletti A, Haraldi I, Momicchioli F (1987) J Phys Chem **91**: 4733
[3] Shim SC, Lee KT, Kim MS (1990) J Org Chem **55**: 4316
[4] Shim SC, Kim MS (1989) J Chem Soc Perkin Trans II, 1897
[5] Jeong BM, Shim SC (1994) J Photochem Photobiol A **79**: 39
[6] Gennari G, Gauzzo G, Gallazzo G (1977) J Phys Chem **81**: 1551
[7] Gajdek P, Becker RS, Elisei F, Mazzucato U, Spalletti A (1996) J Photochem Photobiol A **100**: 57
[8] Spalletti A, Bartocci G, Elisei F, Masetti F, Mazzucato U (1998) Proc Indian Acad Sci **110**: 297
[9] Salamon Z, Skibinski A (1980) Z Naturforsch **35a**: 378
[10] La'cova' M, Chovancova' J, Hy'blova' O, Varkonda SH (1990) Chem Papers **45**: 411
[11] Chula'k I, Sutoris V, Sekerka V (1989) Chem Papers **44**: 131
[12] Papenfuhs T (1987) Chem Abstr **106**: 213936d
[13] El-Daly SA, Fayed TA (1999) Spectrochim Acta (in press)
[14] Demas JN, Crosby GA (1971) J Phys Chem **75**: 1991

[15] Fayed TA (1999) J Photochem Photobiol A **121**: 17
[16] Hatchard JG, Parker CA (1959) Proc Ray Soc London Sec A **235**: 518
[17] Görner H, Schulte-Frohlinde D (1985) J Phys Chem **89**: 4105
[18] Mazzucato U (1982) Pure Appl Chem **54**: 1705
[19] Espenson JH (ed) (1995) Chemical Kinetics and Reaction Mechanisms. McGraw-Hill, New York, p 164
[20] Asano T, Okada T (1984) J Org Chem **49**: 4387

Received February 5, 1999. Accepted (revised) May 3, 1999